

EFFICIENT ADAPTIVE DETECTION THRESHOLD OPTIMIZATION FOR TRACKING MANEUVERING TARGETS IN CLUTTER

J. T. Wang^{*}, H. Q. Wang, Y. L. Qin, and Z. W. Zhuang

College of Electronic Science and Engineering, National University of Defense Technology, Changsha, Hunan 410073, China

Abstract—In this paper, we focus on the adaptive prior detection threshold setting problem to optimize the overall performance of the joint detection-tracking system for maneuvering target tracking in clutter. It is shown that our problem can be reduced to the information reduction factor (IRF) maximization by Gaussian fitting of maneuvering target Markovian switching dynamics via moment matching, even for the case with the nonlinear measurement equation. Our proposed adaptive threshold setting method outperforms the conventional threshold setting approaches greatly and also exhibits a mildly improvement in comparison with the earlier method for this problem in terms of tracking performance, especially in track loss percentage (TLP). However the computational burden of our method is reduced significantly because in our method generally only one IRF corresponding to the common validation region, not the every IRF corresponding to the individual model-conditioned validation region, is needed for threshold optimization at each time step and an approximate closed-form solution can also be obtained for the special case of the Neyman-Pearson (NP) detector.

1. INTRODUCTION

It is well understood that the tracking performance depends significantly on the quality of the measurement data [1, 2], which is provided by the upstream detection subsystem, in terms of both the measurement noise covariance and signal processing parameters, primarily the probabilities of detection and false alarm, when measurement-origin uncertainty occurs [3, 4]. Evidently the detection

Received 17 April 2012, Accepted 13 June 2012, Scheduled 20 June 2012

* Corresponding author: Jian-Tao Wang (wangjiantaonudt@126.com).

and false alarm probabilities, which are absolutely interdependent via the receiver operating characteristic (ROC) curve given the signal-to-noise ratio (SNR), are adjustable. However in the conventional radar or sonar design and processing, detection and tracking subsystems are often treated as the separate entities [5–9] and typically false alarm probability is predetermined and kept constant or selected so that the expected number of false alarms within the validation region equals a predetermined value in consideration of the trade-offs between false alarms and missed detections. The effect of false alarm probability setting on data association performance and tracking error statistics is not accounted for.

Several efforts have been devoted to establishing a link between signal processing subsystem and data processing subsystem. The assumption of the joint detection-tracking system allows a feedback from the downstream tracker to the detector to optimize the overall system performance. Note that detection threshold need not be the actual optimized parameter since detection threshold depends entirely on false alarm probability. In fact false alarm probability is often used as a substitute for detection threshold in the procedure of optimization for convenience sake. In reference [1], the steady-state optimization of detection threshold is investigated by iterating forward the modified Riccati equation (MRE) to convergence and a graphical method is suggested to determine the receiver operating point that optimize tracker performance. However the graphical method is inefficient and also inappropriate for time-varying systems or when the SNR is time varying. To overcome the deficiencies of graphical method, the detection threshold optimization procedure is rigorously formulated and two adaptive detection threshold optimization schemes, namely prior and posterior threshold optimization which depend on measurements up to the previous and current time step respectively, are proposed by minimizing the tracking mean square error (MSE) in [10]. In particular, the prior optimization method requires a single line search for the optimal detection threshold because IRF in the MRE must be evaluated numerically. A satisfactory empirical approximation to IRF in the MRE for a given scenario presented in [11] leads to a closed form solution for the prior threshold optimization scheme in the case of NP detector [12]. It is also demonstrated in reference [13] that the technique of hybrid conditional averaging (HYCA) can be used for adaptive detection threshold optimization. However the studies in references [1, 10, 12, 13] are all preformed for the probabilistic data association filter (PDAF). The prior threshold optimization method is extended to the scenario of maneuvering target tracking [16, 21] in clutter and multiple model (MM) filtering method in [14]. The

simulation results show that track loss percentage (TLP) decreases notably at a cost of increased computational load due to a line search when the proposed extension in [14] is used.

In literature [14], the expected posterior covariance matrix of MM filtering method is evaluated as a weighted sum of that of elemental filters which can be further substituted by either MRE or HYCA approximations. Although this seems reasonable, it is only a heuristic one since the data dependent stochastic terms in the posterior covariance matrix of MM filtering method that accounts for the coupling among the elemental filters is neglected. Another important issue we have to keep in mind is that typical radar epoch duration may allow only a very short time for threshold optimization. In this paper, further focuses are devoted to prior threshold optimization for the maneuvering target tracking in clutter. Our work differs from that in [14] in that we compute the objective function of threshold optimization by approximating the multimodal prior target probability density function with a best-fitting Gaussian (BFG) distribution [15] at each time step to estimate the performance measure for tracking maneuvering targets with linear Markovian switching dynamics. A more reasonable and efficient adaptive detection threshold optimization method for maneuvering target tracking in clutter is proposed and extended to the case with the nonlinear measurement equation. A closed-form solution for the NP detector can be also obtained by the functional approximation to the IRF. Obviously the proper choice of the detection threshold is related to the data association method and the method of tracking evaluation. Efficient use of data from a lowered detection threshold may require the more effective data association methods [17]. The probabilistic data association (PDA) is chosen to select measurements for use in the tracking filter in this work.

The rest of the paper is organized as follows. In Section 2 we describe problem formulation and review some close relevant details of interacting multiple model (IMM) estimator with PDAF modules, i.e., IMMPDAF [18]. In Section 3 we develop the adaptive detection threshold optimization method. The simulation results are presented in Section 4, and some concluding remarks are given in Section 5.

2. PROBLEM FORMULATION

2.1. Target Dynamics and Measurement Model

Consider a discrete-time hybrid system described by the state and observation equations

$$\mathbf{x}(k+1) = \mathbf{F}(k, M_k)\mathbf{x}(k) + \mathbf{G}(k, M_k)\mathbf{v}(k, M_k) \quad (1)$$

$$\mathbf{z}(k) = \mathbf{H}\mathbf{x}(k) + \mathbf{w}(k) \quad (2)$$

with known initial model probabilities and time-homogeneous Markovian transition probability of system modes

$$p_{ij} = P\{M_{k+1} = j | M_k = i\}, \quad \forall i, j \in \mathbf{M}_s \quad (3)$$

where $\mathbf{x}(k)$ is n -dimensional state vector that typically includes position and velocity variables, $\mathbf{z}(k)$ is M -dimensional measurement vector, $\mathbf{v}(k, M_k)$ and $\mathbf{w}(k)$ are mutually uncorrelated zero-mean white Gaussian process and measurement noise vectors with covariance matrices $\mathbf{Q}(k, m_k)$ and $\mathbf{R}(k)$, respectively. The two noise sequences and the initial state are also assumed mutually independent. $\mathbf{F}(k, M_k)$, $\mathbf{G}(k, M_k)$, \mathbf{H} , $\mathbf{Q}(k, m_k)$, $\mathbf{R}(k)$ are assumed known with appropriate dimensions. M_k is modal state (system mode index) which denotes the mode in effect during the time interval between the epoch k and $k+1$, $\mathbf{M}_s \in \{1, 2, \dots, r\}$ is the finite set of all modal states, $P\{\cdot | \cdot\}$ denotes a conditional probability.

In practice, a set of candidate measurements, which are threshold exceedances of matched filter outputs, are provided to the tracking filter due to imperfect target detection and false alarms and only ones in the validation region are considered for updating the target track, namely validated measurements. Ordinarily, the validation region is taken to be an M -dimensional hyperellipsoid centered at the predicted measurement $\hat{\mathbf{z}}(k|k-1)$. Given an arbitrary measurement $\mathbf{z}_l(k)$, it will be in the validation region provided

$$[\mathbf{z}_l(k) - \hat{\mathbf{z}}(k|k-1)]^T \mathbf{S}^{-1}(k) [\mathbf{z}_l(k) - \hat{\mathbf{z}}(k|k-1)] \leq g^2 \quad (4)$$

where $\mathbf{S}(k)$ is the covariance of the predicted measurement, g , referred to as the number of sigmas for the gate, is the threshold for ensuring that the target-originated measurement falling inside the validation region with a probability of P_G if detected. The volume of validation region is given by

$$V(k) = c_M g^M |\mathbf{S}(k)|^{\frac{1}{2}} \quad (5)$$

where $c_M = \pi^{M/2} / \Gamma(M/2 + 1)$, with $\Gamma(\cdot)$ being gamma function, is the volume of the M -dimensional unit hypersphere.

Let $\mathbf{Z}^k = \{\mathbf{z}_l(k)\}_{l=1}^{m_k}$ denote the set of validated measurements at time step k , where m_k is number of validated measurements. The true measurement originated from the target of interest may be among \mathbf{Z}^k with detection probability. A typical model for false alarm measurements is that they are uniformly spatially distributed within the validation region and independent across time assuming that the

number of them accords with a Poisson distribution with mean $\lambda V(k)$, where λ is the spatial clutter density. The relationship between λ and false alarm probability P_{fa} can be expressed by

$$\lambda(k)V(k) = P_{fa}(k)N_c(k) = P_{fa}(k)\frac{V(k)}{V_c} \quad (6)$$

where $N_c(k) = V(k)/V_c$, with V_c being the volume of resolution cell, is number of resolution cells enclosed by the common validation region. Then it follows that $\lambda(k) = P_{fa}(k)/V_c$.

2.2. IMMPDFAF Estimator

The optimal estimator for above hybrid system has exponentially increasing complexity with respect to time due to the need to consider all “histories” [19]. For the problem considered here, IMMPDFAF, a well-known suboptimal (yet practical) multiple model filter, is employed to estimate the target state in this paper. For r models in the IMMPDFAF, there will be r validation regions, one for each model, and r sets of validation measurements. Thus a common validation region is necessary to compute the model-conditioned likelihoods. A common validation region can be obtained by taking the union of the r sets of model-conditioned validation regions. Typically the “largest” innovation covariance matrix corresponding to “noisiest” model covers the others and therefore can be used in (4) and (5) to determine the common validation region [18]. For the details and steps of the IMMPDFAF, see reference [22].

2.3. Prior Detection Threshold Optimization

Prior detection threshold optimization problem can be formulated as follows. We attempt to minimize an objective function, e.g., the tracking mean square errors (MSE), by seeking an optimum operating false alarm probability. However when this optimization is carried out, we have no access to the observation and the target state at the next sampling instant. We therefore have to minimize its expected value, that is, we select an operating false alarm probability such that

$$P_{fa}^* = \arg \min_{P_{fa}} \left\{ E \left\{ \|\mathbf{M}[\mathbf{x}(k+1) - \hat{\mathbf{x}}(k+1|k+1)]\|^2 | \mathbf{Z}^k \right\} \right\},$$

subject to $P_d = f_{\text{ROC}}(P_{fa}, \eta)$ and $0 \leq P_{fa} \leq 1$ (7)

where \mathbf{M} is a positive semi-definite weighting matrix that ensures the units of the objective function are consistent [23] or is used to facilitate individual component penalization, η is SNR and f_{ROC} denotes the ROC curve that links P_{fa} with P_d .

The objective function can be rewritten as

$$\begin{aligned}
 J(P_{fa}) &= E \left\{ \left\| \mathbf{M} [\mathbf{x}(k+1) - \hat{\mathbf{x}}(k+1|k+1)] \right\|^2 \middle| \mathbf{Z}^k \right\} \\
 &= E \left\{ \text{tr} \left[\mathbf{M} \mathbf{P}(k+1|k+1) \mathbf{M}^T \right] \middle| \mathbf{Z}^k \right\} \\
 &= \text{tr} \left\{ E \left[\mathbf{M} \mathbf{P}(k+1|k+1) \mathbf{M}^T \middle| \mathbf{Z}^k \right] \right\} \\
 &= \text{tr} \left\{ \mathbf{M} E \left[\mathbf{P}(k+1|k+1) \middle| \mathbf{Z}^k \right] \mathbf{M}^T \right\} \tag{8}
 \end{aligned}$$

where $\text{tr}\{\cdot\}$ is the trace operator. Equation (8) shows that the key point to quantify the utility of a particular operating P_{fa} is the calculation of the expected posterior covariance matrix of the state estimator since it contains all information to evaluate the objective function. The posterior covariance matrix $\mathbf{P}(k+1|k+1)$ of IMM-PDAF is measurement dependent. And hence evaluation of its expected value, i.e., its predictive value, without recourse to time-consuming Monte Carlo simulations is quite difficult due to the coupling between the elemental filters and three types of uncertainties involved: the continuous-valued uncertainty in target states, the discrete-valued uncertainties in switching modal state and in the origin of the measurements. However we will show that the problem can be converted into a tractable one by considering Gaussian approximation to the target dynamics.

3. ADAPTIVE DETECTION THRESHOLD OPTIMIZATION

3.1. Gaussian Fitting of Target Dynamics Via Moment Matching

The dynamics of the linear jump Markov system described by (1) can be approximated, using moment matching [20], by that of a linear Gaussian system that obeys a single model

$$\mathbf{x}(k+1) \approx \mathbf{\Phi}(k) \mathbf{x}(k) + \boldsymbol{\varepsilon}(k) \tag{9}$$

for all time steps, where $\boldsymbol{\varepsilon}(k)$ is zero-mean white Gaussian noise vectors with covariance $\mathbf{Q}_{\boldsymbol{\varepsilon}}(k)$. $\mathbf{\Phi}(k)$ and $\boldsymbol{\varepsilon}(k)$ are chosen so that at each time step the distribution of $\mathbf{x}(k+1)$ has the same mean and covariance under each system. Although it is clearly that the above approximation does not fully capture the characteristics of the distribution of the true target state, which may be multi-modal due to model switching, it is demonstrated in [15] that the corresponding moment-matched state distribution fits the true distribution well and

can be used to provide predictive measures that is in close agreement with the performance of state-of-the-art multiple model estimator with a very low computational load, which is important in time critical scenarios.

Let $M^j(k)$ denote the event that $M_k = j$, the predicted model probability $\mu^j(k + 1|k)$ can be computed by

$$\mu^j(k + 1|k) = P\{M^j(k + 1)|\mathbf{Z}^k\} = \sum_{i=1}^r p_{ij}P\{M^i(k)|\mathbf{Z}^k\}. \quad (10)$$

Using the total probability theorem, we can obtain

$$\begin{aligned} & E \left[x(k + 1) \middle| \mathbf{Z}^k \right] \\ &= \sum_{j=1}^r E \left[\mathbf{x}(k + 1) \middle| M^j(k + 1), \mathbf{Z}^k \right] P \left\{ M^j(k + 1) \middle| \mathbf{Z}^k \right\} \\ &= \sum_{j=1}^r \mathbf{F}(k, M_k^j) E \left[\mathbf{x}(k) \middle| \mathbf{Z}^k \right] \mu^j(k + 1|k) \\ &= \sum_{j=1}^r \mathbf{F}(k, M_k^j) \mu^j(k + 1|k) \cdot E \left[\mathbf{x}(k) \middle| \mathbf{Z}^k \right] \end{aligned} \quad (11)$$

for the linear jump Markov system. And trivially for the single model system expressed by (9), we have

$$E \left[\mathbf{x}(k + 1) \middle| \mathbf{Z}^k \right] = \Phi(k) \cdot E \left[\mathbf{x}(k) \middle| \mathbf{Z}^k \right] \quad (12)$$

$$Cov \left[\mathbf{x}(k + 1) \middle| \mathbf{Z}^k \right] = \Phi(k) Cov \left[\mathbf{x}(k) \middle| \mathbf{Z}^k \right] \Phi^T(k) + \mathbf{Q}_\varepsilon(k). \quad (13)$$

It follows that

$$\Phi(k) = \sum_{j=1}^r \mathbf{F} \left(k, M_k^j \right) \mu^j(k + 1|k) \quad (14)$$

and

$$\mathbf{Q}_\varepsilon(k) = Cov \left[\mathbf{x}(k + 1) \middle| \mathbf{Z}^k \right] - \Phi(k) Cov \left[\mathbf{x}(k) \middle| \mathbf{Z}^k \right] \Phi^T(k). \quad (15)$$

Note that the single model system described by (9) is merely utilized for efficiently calculating the specified objective function and determining the detection threshold to optimize the performance of the joint detection-tracking system, while the state estimator still relies on the linear jump Markov system given by (1). So, to calculate $\Phi(k)$ and $\mathbf{Q}_\varepsilon(k)$, $\mu^j(k + 1|k)$ in (14) and $Cov \left[\mathbf{x}(k) \middle| \mathbf{Z}^k \right]$ in (15) can

be replaced with the corresponding filter-calculated value obtained from the procedure of state inference. $Cov[\mathbf{x}(k+1)|\mathbf{Z}^k]$ can be approximated by the error variance of the combined model-conditioned state prediction, which can be obtained according to the Gaussian mixture equations:

$$\begin{aligned} Cov[\mathbf{x}(k+1)|\mathbf{Z}^k] &= \mathbf{P}(k+1|k) \\ &= \sum_{j=1}^r \mu^j(k+1|k) \{ \mathbf{P}^j(k+1|k) \\ &\quad + [\hat{\mathbf{x}}^j(k+1|k) - \hat{\mathbf{x}}(k+1|k)] [\hat{\mathbf{x}}^j(k+1|k) - \hat{\mathbf{x}}(k+1|k)]^T \} \end{aligned} \quad (16)$$

$$\hat{\mathbf{x}}(k+1|k) = \sum_{j=1}^r \hat{\mathbf{x}}^j(k+1|k) \mu^j(k+1|k) \quad (17)$$

where $\hat{\mathbf{x}}(k+1|k)$ is the combined state prediction, $\hat{\mathbf{x}}^j(k+1|k)$, and $\mathbf{P}^j(k+1|k)$ denote model-conditioned state prediction and associated error variance. The calculations of $\hat{\mathbf{x}}(k+1|k)$ and $\mathbf{P}(k+1|k)$ can be inserted into the IMMPDAF procedure naturally, though they are not parts of the IMMPDAF algorithm recursions.

3.2. Solution to Adaptive Detection Threshold Optimization

For the linear Gaussian system described by the state Equation (9) and observation Equation (2), MRE [1] (modified Riccati equation) and HYCA [24] (hybrid conditional averaging) technologies are available at the time step k for quantifying the effect of measurement-origin uncertainty and provide two methods to obtain a deterministic approximation for the predicted posterior covariance matrix at the next time step when the PDA is used. MRE is obtained by replaced the measurement dependent terms with their conditional expectations over both the locations and the numbers of possible validated measurements in the covariance update recursion equation. And it differs from the original Riccati equation only by multiplying a scalar information reduction factor. Since MRE yields a significantly simpler global averaging approximation to the posterior covariance matrix update, MRE is used here to calculate the objective function efficiently. For the case of MRE, the expected posterior covariance matrix in (8) can be approximated by [1]

$$\begin{aligned} &E[\mathbf{P}(k+1|k+1)|\mathbf{Z}^k] \\ &\cong \mathbf{P}(k+1|k) - q_2(P_{fa}(k+1)) \mathbf{K}(k+1) \mathbf{S}(k+1) \mathbf{K}^T(k+1) \end{aligned} \quad (18)$$

where $\mathbf{S}(k + 1) = \mathbf{HP}(k + 1|k)\mathbf{H}^T + \mathbf{R}(k)$, $\mathbf{K}(k + 1) = \mathbf{P}(k + 1|k)\mathbf{H}^T\mathbf{S}^{-1}(k + 1)$ is Kalman filter gain for the system described by Equations (9) and (2), $q_2(P_{fa}(k + 1))$ is IRF and lies between 0 and 1. The P_{fa} dependent expression for $q_2(P_{fa}(k + 1))$ follows directly from [1, 12], namely

$$\begin{aligned}
 q_2(P_{fa}(k + 1)) &= \frac{P_d(k + 1)c_M}{(2\pi)^{M/2}} \\
 &\cdot \sum_{m_{k+1}=1}^{\infty} \frac{e^{-P_{fa}(k+1)N_c(k+1)} [P_{fa}(k + 1)N_c(k + 1)]^{m_{k+1}-1}}{(m_{k+1} - 1)!} \\
 &\cdot \left(\frac{M}{g^M}\right)^{m_{k+1}-1} I_2(P_{fa}(k + 1), m_{k+1}) \tag{19}
 \end{aligned}$$

with

$$\begin{aligned}
 &I_2(P_{fa}(k + 1), m_{k+1}) \\
 &= \int_0^g \dots \int_0^g \frac{\exp(-r_1^2)r_1^2}{b(P_{fa}(k + 1)) + \sum_{j=1}^{m_{k+1}} \exp(-r_j^2/2)} \\
 &\cdot (r_1 r_2 \dots r_{m_{k+1}})^{M-1} dr_1 dr_2 \dots dr_{m_{k+1}} \tag{20}
 \end{aligned}$$

$$b(P_{fa}(k + 1)) = (2\pi)^{M/2} \frac{P_{fa}(k + 1)N_c(k + 1)}{c_M g^M} \cdot \frac{[1 - P_d(k + 1)P_G]}{P_d(k + 1)} \tag{21}$$

Substituting Equation (18) into Equation (8) and simplifying yields

$$\begin{aligned}
 J(P_{fa}) &= tr [\mathbf{MP}(k + 1|k)\mathbf{M}^T] \\
 &- q_2(P_{fa}(k + 1)) tr [\mathbf{MK}(k + 1)\mathbf{S}(k + 1)\mathbf{K}^T(k + 1)\mathbf{M}^T] \tag{22}
 \end{aligned}$$

It can be seen from Equation (22) that $q_2(P_{fa}(k + 1))$ is the only term that depends on $P_{fa}(k + 1)$. Since $\mathbf{MK}(k + 1)\mathbf{S}(k + 1)\mathbf{K}^T(k + 1)\mathbf{M}^T \geq 0$ implies $tr [\mathbf{MK}(k + 1)\mathbf{S}(k + 1)\mathbf{K}^T(k + 1)\mathbf{M}^T] \geq 0$, $J(P_{fa})$ will be minimized by maximizing $q_2(P_{fa}(k + 1))$. Thus our problem becomes

$$\begin{aligned}
 P_{fa}^* &= \arg \max_{P_{fa}} \{q_2(P_{fa}(k + 1))\}, \\
 &\text{subject to } P_d = f_{ROC}(P_{fa}, \eta) \text{ and } 0 \leq P_{fa} \leq 1 \tag{23}
 \end{aligned}$$

which has the same form as in [10, 12] though our focuses are on the detection threshold optimization for tracking maneuvering target in clutter and a weighting matrix is considered to equalize the components in the tracking MSE. Note that in essence the final form of the detection

threshold optimization for maneuvering targets tracking in clutter in reference [14] is maximization of a weighting sum of model-conditioned IRFs, which are different only due to different model-conditioned validation regions. However the actual effective validation region is the common one in IMM-PDAF estimator, which makes our proposal of (23) seem more reasonable.

We cannot solve (23) analytically because evaluation of IRF given by Equation (19) has to be performed numerically since m_k -fold integration is involved, e.g., Monte Carlo integration scheme. However a satisfactory empirical approximation for $q_2(P_{fa}(k+1))$ suggested by [11] can be used to further simplify our analysis. In the case of $M = 2$ and $g = 4$, $q_2(P_{fa}(k+1))$ can be approximated by

$$q_2(P_{fa}(k+1)) \cong \frac{0.997P_d(k+1)}{1 + 0.37[P_d(k+1)]^{-1.57}P_{fa}(k+1)N_c(k+1)} \quad (24)$$

where $\lambda(k)V(k) = P_{fa}(k)N_c(k)$ is used. To find the single maximum of strictly unimodal [10] $q_2(P_{fa}(k+1))$, we can set the derivative of $q_2(P_{fa}(k+1))$ with respect to $P_{fa}(k+1)$ equal to zero recalling some specific ROC curve for various types of detectors. For the case of NP detector whose ROC curve is expressed by

$$P_d = (P_{fa})^{\frac{1}{1+\eta}}, \quad (25)$$

the optimum false alarm probability for the problem described by Equation (23) is given by [12]

$$P_{fa}(k+1) = \begin{cases} [0.37N_c(k+1)(\eta - 1.57)]^{\frac{1+\eta}{0.57-\eta}}, & \eta \geq 1.57 + \frac{1}{0.37N_c(k+1)} \\ 1, & \text{otherwise.} \end{cases} \quad (26)$$

Note that the optimum operating false alarm probability is suggested to be equal to 1 under the condition of $\eta < 1.57 + 1/[0.37N_c(k+1)]$, that is, the track before detect (TBD) approach [25] is suggested for the case of extreme low SNR.

3.3. Extension to the Case With the Nonlinear Measurement Equation

When measurement equation involves nonlinearities, e.g., range and range rate are provided to the tracker [23], the unscented Kalman filter (UKF), which exhibits many performance improvements over the extended Kalman filter (EKF), can be used as elemental filter in the IMM algorithm. However PDA can still be used to deal with the

measurement-origin uncertainty. Then the measurements that are not target-originated still increase the covariance of the state estimate. It has been shown that the expected posterior covariance matrix of the state in this scenario can be given by [23]

$$E\left[\mathbf{P}(k+1|k+1)|\mathbf{Z}^k\right] \cong \mathbf{P}(k+1|k) - q_2(P_{fa}(k+1))\mathbf{P}^c(k+1|k+1) \quad (27)$$

where $\mathbf{P}^c(k+1|k+1)$ is a covariance reduction that reduces the uncertainty in the prediction covariance due to the true target-originated measurement, which can be obtained using the unscented transform and is given by

$$\mathbf{P}^c(k+1|k+1) = \mathbf{P}_{xz}(k+1|k)\mathbf{S}^{-1}(k+1)\mathbf{P}_{xz}^T(k+1|k) \quad (28)$$

where $\mathbf{P}_{xz}(k+1|k)$ is the cross covariance between the predicted state and the predicted measurement. Clearly $\mathbf{P}^c(k+1|k+1)$ is independent of the measurement value and the false alarm probability. $q_2(P_{fa}(k+1))$ is still the only term that depends on the false alarm probability. Thus the problem of the detection threshold optimization reduces to (23) again. But the dimension of measurement vector may be not equal to 2, and then the existence of the satisfactory analytic functional approximation for IRF is still an open problem. Therefore a close-form solution to the optimum alarm probability may not exist. In general, a line search algorithm that requires only the values of the objective function, such as Golden-Section or Fibonacci Search methods, can be applied to solve (23) [10].

Recalling the results in [10, 12], an interesting conclusion can be summarized. That is, the detection threshold optimization is equivalent to IRF maximization for single target tracking in clutter, no matter how the target dynamics evolve and whether the measurement equation is linear. It seems that IRF elegantly and effectively quantifies the information reduction due to the measurement-origin uncertainty and missed data. The smaller it is, the greater the degradation of the estimation performance is.

4. SIMULATION RESULTS

A maneuvering target tracking scenario in air traffic control (ATC) that is very similar to the one in [14] is considered for comparisons among our method, the method proposed in [14] (referred to as “method 2”) and the conventional detection threshold setting methods where the operating false alarm probability are fixed. Here, an aircraft flies straight for 90 s in the (x, y) plane, starting from (13 500 m, 8 594 m) with an initial velocity (0 m/s, 150 m/s) at time $t = 0$ s. And then it executes a 90° right turn with turn rate of 1°/s (which amounts to

an acceleration of 0.26 g at this speed). The center of the coordinated turn is approximately the location of the radar. After the turn, the aircraft continues straight at the constant velocity for 120 s. The target trajectory is shown in Fig. 1. The radar with an NP detector, located at $(0 \text{ m}, 0 \text{ m})^T$, provides direct position only measurements (after the polar-to-Cartesian conversion) for every sampling period $T = 3 \text{ s}$ with a rectangular resolution cell of 50 m in each coordinate. Assuming the true measurement is uniformly distributed within the resolution cell that registers a hit [22], the covariance of measurement noise is

$$\mathbf{R}(k) = \begin{bmatrix} (\Delta r_x / \sqrt{12})^2 & 0 \\ 0 & (\Delta r_y / \sqrt{12})^2 \end{bmatrix} \quad (29)$$

where Δr_x and Δr_y , both assumed to be equal to 50 m, are resolutions in x and y directions, respectively.

For the true dynamics, the constant velocity uniform motion (UM) is implemented as a white noise acceleration (WNA) [20] model with low level process noise due to winds, etc. and the maneuver (turn) is obtained via a coordinated turn (CT) [20] model with a constant turn rate. In both WNA and CT models, the standard covariance of process noise is assumed to be 0.01 m/s^2 for the linear portion of the state transition.

The range-dependent SNR at the radar is modeled according to

$$\eta(r) = \left(\frac{r_0}{r}\right)^4 \eta_0 \quad (30)$$

where r is the range between the target and the radar, η_0 is the SNR for the target at the range r_0 . Note that all other factors except range in the SNR equation are assumed to be constant in the simulation and

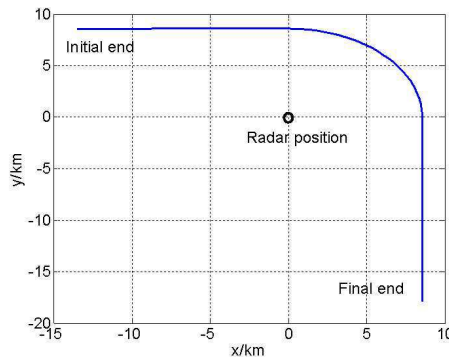


Figure 1. The target trajectory.

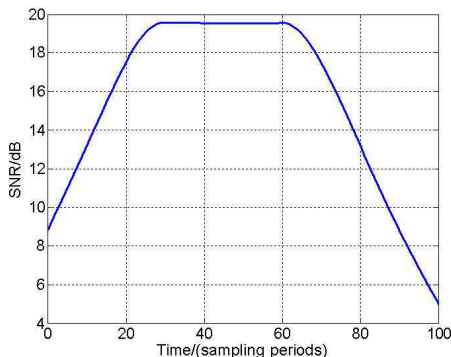


Figure 2. The SNR evolving over time for $r_0^4\eta_0 = 0.5 \times 10^{18} \text{ m}^4$.

their effects are accounted by $r_0^4\eta_0$ for simplicity. The SNR evolving over time is illustrated in Fig. 2 for $r_0^4\eta_0 = 0.5 \times 10^{18} \text{ m}^4$ †.

The IMMPDAF estimator used in this scenario consists of two elemental PDAFs corresponding to the nonmaneuvering mode (mode 1) and maneuvering mode (mode 2), which both use WNA model and differ only in the process noise levels. The one with the lower noise level with standard deviation 0.01 m/s^2 is used to model the uniform motion and the other one with standard deviation 3 m/s^2 for the maneuver. The initial mode probabilities are set to be 0.5 equally. Note that the mode transition probabilities have an impact on the peak estimation errors at the onset of the maneuver and the estimation errors during the uniform motion. They are suggested in [20] to be matched with the mean sojourn time in units of the sampling interval in each mode. Here, the mode transition probability matrix is designed to be

$$\pi = \begin{bmatrix} 0.99 & 0.01 \\ 0.03 & 0.97 \end{bmatrix}. \tag{31}$$

For the conventional detection threshold setting method, typical false alarm probability values of 10^{-8} , 10^{-6} , 10^{-4} , 10^{-2} are used and kept constant in the simulations. 500 Monte Carlo runs are performed for each considered method.

The comparisons of the various detection threshold setting methods in terms of tracking performance metrics are shown in Table 1 and Fig. 3 ~ Fig. 4 for $r_0^4\eta_0 = 0.5 \times 10^{18} \text{ m}^4$. A track is accepted as a lost track when the average estimation error for that Monte Carlo run exceeds the measurement error [14]. All estimation errors are

† The scenarios with other different values of $r_0^4\eta_0$ are also investigated, however the similar results are obtained and not presented here for brevity.

Table 1. The tracking performance for the various detection threshold setting methods.

	TLP/%	Average position RMSE/m	Average velocity RMSE/m/s	Maneuver detection delay/scans	Average UM probability error
Our method	54	17.1642	3.9281	2	0.1257
Method 2	59	17.2507	3.9177	2	0.1262
$P_{fa} = 10^{-8}$	100	—	—	—	—
$P_{fa} = 10^{-6}$	99	17.7932	3.8554	2	0.1366
$P_{fa} = 10^{-4}$	85	18.1244	4.1469	2	0.1304
$P_{fa} = 10^{-2}$	71	17.4399	3.9644	2	0.1236

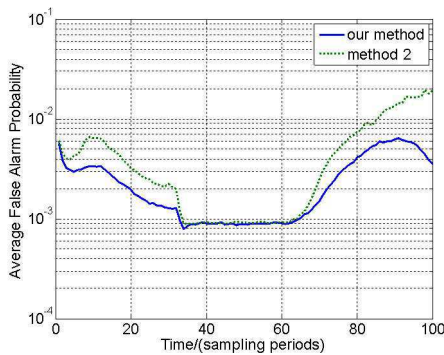


Figure 3. The optimum false alarm probabilities suggested by adaptive detection threshold optimization scheme.

obtained from Monte Carlo runs for which the track is converged. The root mean squared errors (RMSEs) of position and velocity estimation are coordinate-combined. The average position/velocity RMSE is calculated by taking the mean of the position/velocity RMSEs through all time steps. The maneuver detection delay, measured in sampling periods, is defined to be the latency from the maneuver onset time to the time when the probability of the mode 2 exceeds 0.5. Average UM probability error denotes the average mode 2 probability when the target is in uniform motion (mode 1). The following observations can be made:

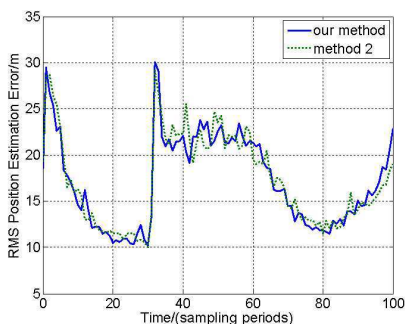
1) Compared with the conventional threshold setting method, the TLP decreases significantly when the adaptive detection threshold optimization scheme is used. However the position and velocity RMSEs only exhibit marginal reductions, which is probably because the tracks

that have considerable estimation errors are recognized as lost ones and have not been taken into account during calculating the errors.

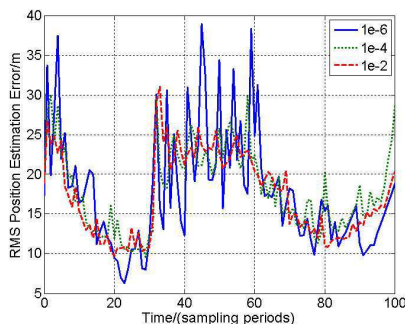
2) When SNR is at a high level, the optimum false alarm probability should decrease as SNR increases and vice versa. However our proposed method for dynamic threshold setting also suggests the optimum value of P_{fa} decrease mildly as SNR continues decreasing when the sufficiently low SNR is reached, as can be seen from Fig. 3. In fact, this reflects the requirement that the number of false alarm measurements, potentially corrupting the track, should be limited due to low detection probability on a low SNR [17]. Note that this trend also cannot hold, i.e., the optimum P_{fa} should still be increased in the extremely difficult SNR scenarios.

3) The optimum P_{fa} should decrease when the target is in the maneuver mode. Since the volume of validation region increases due to the larger estimation errors of the estimator during maneuvers, this seems reasonable to avoid the track loss.

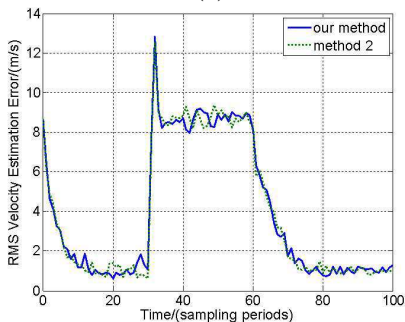
4) The detection threshold setting has imperceptible effect on the maneuver detection capability and mode estimation error, which is true at least in the scenario considered.



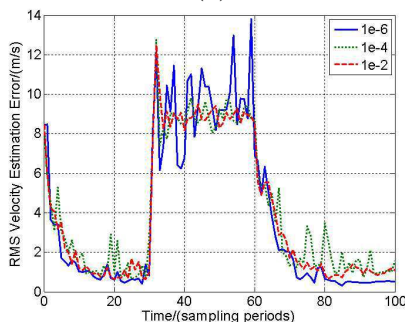
(a)



(b)



(c)



(d)

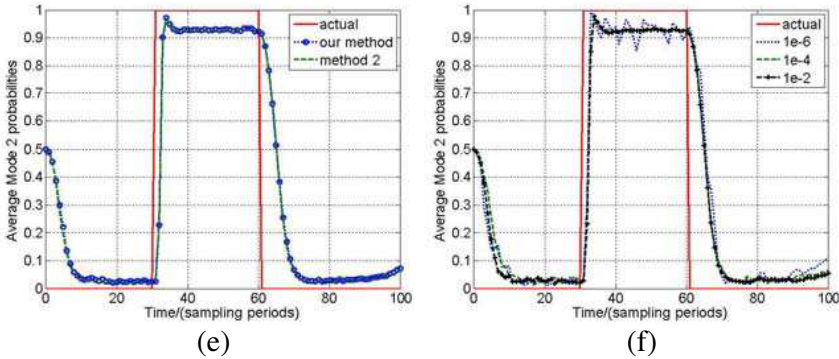


Figure 4. Comparisons of coordinate-combined position RMSEs, velocity RMSEs and mode 2 probabilities for the adaptive and conventional detection threshold setting methods. (a) Position RMSEs for adaptive threshold scheme. (b) Position RMSEs for constant threshold scheme. (c) Velocity RMSEs for adaptive threshold scheme. (d) Velocity RMSEs for constant threshold scheme. (e) Mode 2 probabilities for adaptive threshold scheme. (f) Mode 2 probabilities for constant threshold scheme.

5) Our proposed adaptive detection threshold optimization method is immoderately better than method 2 in terms of tracking performance metrics, but the computational load is dramatically reduced since only one IRF corresponding to the common validation region is needed for threshold optimization and no search is involving for the special case of the NP detector. Furthermore, our method suggests a lower optimum false alarm probability, which implies fewer false alarm measurements, relative to method 2 at almost every time step, which makes our method more appealing in view of the computational capacity of radar processor in handling the number of false alarm measurements.

5. CONCLUSION

We have investigated the adaptive prior detection threshold optimization for tracking the maneuvering targets with linear Markovian switching dynamics in clutter to improve the overall performance of the joint detection-tracking system in the paper. Previous work for this problem suggested maximization of a weighting sum of all model-conditioned IRFs to search for the optimum threshold [14]. A more reasonable and efficient method is proposed and extended to the scenario with the nonlinear measurement equation. It is shown that the

computational burden of our method is reduced significantly with slight improvements in tracking performance, especially in terms of TLP.

Note that uncertainty in the estimate of target SNR may preclude use of an optimal threshold based on target SNR [17]. However the same can be said for the constant false alarm rate (CFAR) approaches which also need the target SNR to determine the receiver operating point. A practical approach is to use the measured target SNR for the adaptive threshold setting (maybe not the best) given that the SNR is monitored. Future work includes scheduling the radar waveform in addition to detection threshold so as to optimize the overall tracking performance since the transmitted waveform is crucial for the measurement accuracy.

REFERENCES

1. Fortmann, T. E., Y. Bar-Shalom, M. Scheffe, and S. Gelfand, "Detection thresholds for tracking in clutter-A connection between estimation and signal processing," *IEEE Transactions on Automatic Control*, Vol. 30, No. 3, 221–229, 1985.
2. Kural, F., F. Arıkan, O. Arıkan, and M. Efe, "Performance evaluation of track association and maintenance for a MFPAR with doppler velocity measurements," *Progress In Electromagnetics Research*, Vol. 108, 249–275, 2010.
3. Bar-Shalom, Y., F. Daum, and J. Huang, "The probabilistic data association filter," *IEEE Control Systems Magazine*, Vol. 29, No. 6, 82–100, 2009.
4. Hong, S., L. Wang, Z. G. Shi, and K. S. Chen, "Simplified particle PHD filter for multiple-target tracking: Algorithm and architecture," *Progress In Electromagnetics Research*, Vol. 120, 481–498, 2011.
5. Niu, R., P. Willett, and Y. Bar-Shalom, "Tracking considerations in selection of radar waveform for range and range-rate measurements," *IEEE Transactions on Aerospace and Electronics Systems*, Vol. 38, No. 2, 2002.
6. Wang, Q., J. Li, M. Zhang, and C. Yang, "H-infinity filter based particle filter for maneuvering target tracking," *Progress In Electromagnetics Research B*, Vol. 30, 103–116, 2011.
7. Hatam, M., A. Sheikhi, and M. A. Masnadi-Shirazi, "Target detection in pulse-train MIMO radars applying ICA algorithms," *Progress In Electromagnetics Research*, Vol. 122, 413–435, 2012.
8. Wang, X., J. F. Chen, Z. G. Shi, and K. S. Chen, "Fuzzy-control-

- based particle filter for maneuvering target tracking,” *Progress In Electromagnetics Research*, Vol. 118, 1–15, 2011.
9. Chen, J. F., Z. G. Shi, S. H. Hong, and K. S. Chen, “Grey prediction based particle filter for maneuvering target tracking,” *Progress In Electromagnetics Research*, Vol. 93, 237–254, 2009.
 10. Gelfand, S. B., T. E. Fortmann, and Y. Bar-Shalom, “Adaptive detection threshold optimization for tracking in clutter,” *IEEE Transactions on Aerospace and Electronics Systems*, Vol. 32, No. 2, 1996.
 11. Kershaw, D. J. and R. J. Evans, “A contribution to performance prediction for probabilistic data association tracking filters,” *IEEE Transactions on Aerospace and Electronics Systems*, Vol. 32, No. 3, 1143–1148, 1996.
 12. Aslan, M. S., A. Saranlı, and B. Baykal, “Tracker-aware adaptive detection: An efficient closed-form solution for the Neyman-Pearson case,” *Digital Signal Processing*, Vol. 20, No. 5, 1468–1481, 2010.
 13. LI, X. R. and Y. Bar-Shalom, “Detection threshold selection for tracking performance optimization,” *IEEE Transactions on Aerospace and Electronics Systems*, Vol. 30, No. 3, 1994.
 14. Aslan, M. S. and A. Saranlı, “A tracker-aware detector threshold optimization formulation for tracking maneuvering targets in clutter,” *Signal Processing*, Vol. 91, No. 9, 2213–2221, 2011.
 15. Hernandez, M., B. Ristic, A. Farina, T. Sathyan, and T. Kirubarajan, “Performance measure for Markovian switching systems using best-fitting Gaussian distributions,” *IEEE Transactions on Aerospace and Electronic Systems*, Vol. 44, No. 2, 724–747, 2008.
 16. Bi, S. and X. Y. Ren, “Maneuvering target doppler-bearing tracking with signal time delay using interacting multiple model algorithms,” *Progress In Electromagnetics Research*, Vol. 87, 15–41, 2008.
 17. Blackman, S. and R. Popoli, *Design and Analysis of Modern Tracking Systems*, Artech House, Boston, London, 1999.
 18. Kirubarajan, T., Y. Bar-Shalom, W. D. Blair, and G. A. Watson, “IMMPDAF for radar management and tracking benchmark with ECM,” *IEEE Transactions on Aerospace and Electronic Systems*, Vol. 34, No. 4, 1115–1134, 1998.
 19. Bar-Shalom, Y. and T. E. Fortmann, *Tracking and Data Association*, Academic Press, New York, 1988.
 20. Bar-Shalom, Y., X. R. Li, and T. Kirubarajan, *Estimation with Applications to Tracking and Navigation*, John Wiley & Sons, Inc.,

New York, 2001.

21. Shi, Z. G., S. H. Hong, and K. S. Chen, "Tracking airborne targets hidden in blind doppler using current statistical model particle filter," *Progress In Electromagnetics Research*, Vol. 82, 227–240, 2008.
22. Bar-Shalom, Y. and X. R. Li, *Multitarget-Multisensor Tracking: Principles and Technique*, YBS Publishing, Storrs, CT, 1995.
23. Sira, S. P., A. Papandreou-Suppappola, and D. Morrell, "Dynamic configuration of time-varying waveforms for agile sensing and tracking in clutter," *IEEE Transactions on Signal Processing*, Vol. 55, No. 7, 3207–3217, 2007.
24. Li, X. R. and Y. Bar-Shalom, "Stability evaluation and track life of the PDAF for tracking in clutter," *IEEE Transactions on Automatic Control*, Vol. 36, No. 5, 588–602, 1991.
25. Buzzi, S., M. Lops, and L. Venturino, "Track-before-detect procedures for early detection of moving target from airborne radars," *IEEE Transactions on Aerospace and Electronic Systems*, Vol. 41, No. 3, 937–954, 2005.